

**Molecular Cell, Volume 75**

**Supplemental Information**

**Osh Proteins Control Nanoscale Lipid Organization**

**Necessary for PI(4,5)P<sub>2</sub> Synthesis**

**Taki Nishimura, Michael Gecht, Roberto Covino, Gerhard Hummer, Michal A. Surma, Christian Klose, Hiroyuki Arai, Nozomu Kono, and Christopher J. Stefan**

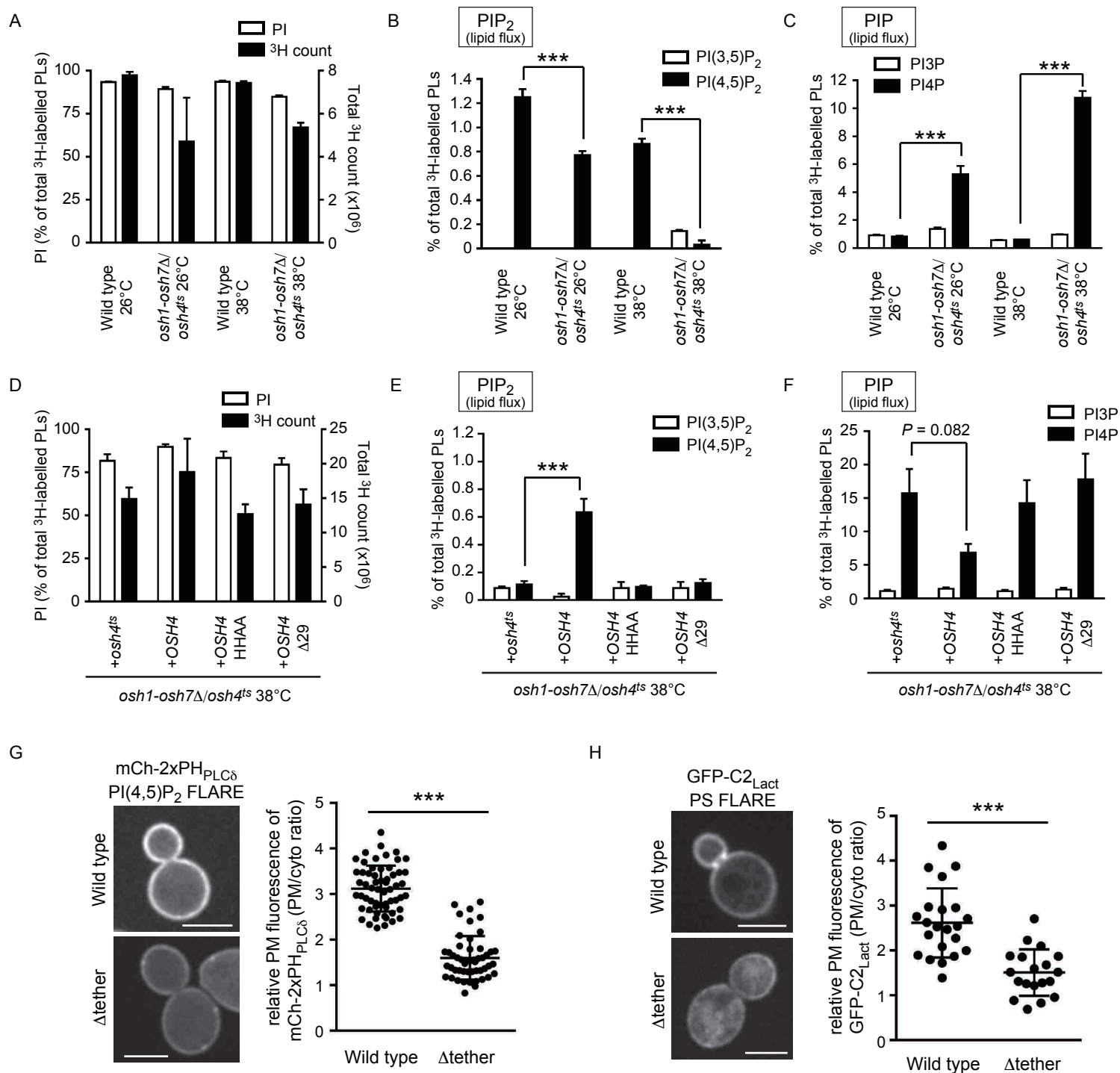


**Figure S1. Reduction of PI(4,5)P<sub>2</sub> and PS levels at the PM of *osh1-7Δ/osh4<sup>ts</sup>* and Δtether mutants, related to Figure 1 and the Supplemental Data Set**

(A-C) Measurements of phosphatidylinositol (PI) and phosphoinositide lipid metabolism by <sup>3</sup>H-inositol labeling and HPLC analysis of wild type and *osh1-7Δ/osh4<sup>ts</sup>* cells cultured at 26°C or 38°C for 1 h. Data represent mean ± SEM (n = 3). (D-F) Measurements of phosphatidylinositol (PI) and phosphoinositide lipid metabolism by <sup>3</sup>H-inositol labeling and HPLC analysis of *osh1-7Δ/osh4<sup>ts</sup>* cells expressing wild type or mutant forms of Osh4 cultured at 38°C for 1 h. Data represent mean ± SEM (n = 3). (G, H) PI(4,5)P<sub>2</sub> (mCherry-2xPH<sub>PLCδ</sub>) and PS (GFP-C2<sub>Lact</sub>) FLARE localization in wild type and Δtether cells. Data represent mean ± SD; (G) n ≥ 50 cells, (H) n ≥ 19 cells. Scale bars, 4 μm. \*\*\*P < 0.001.

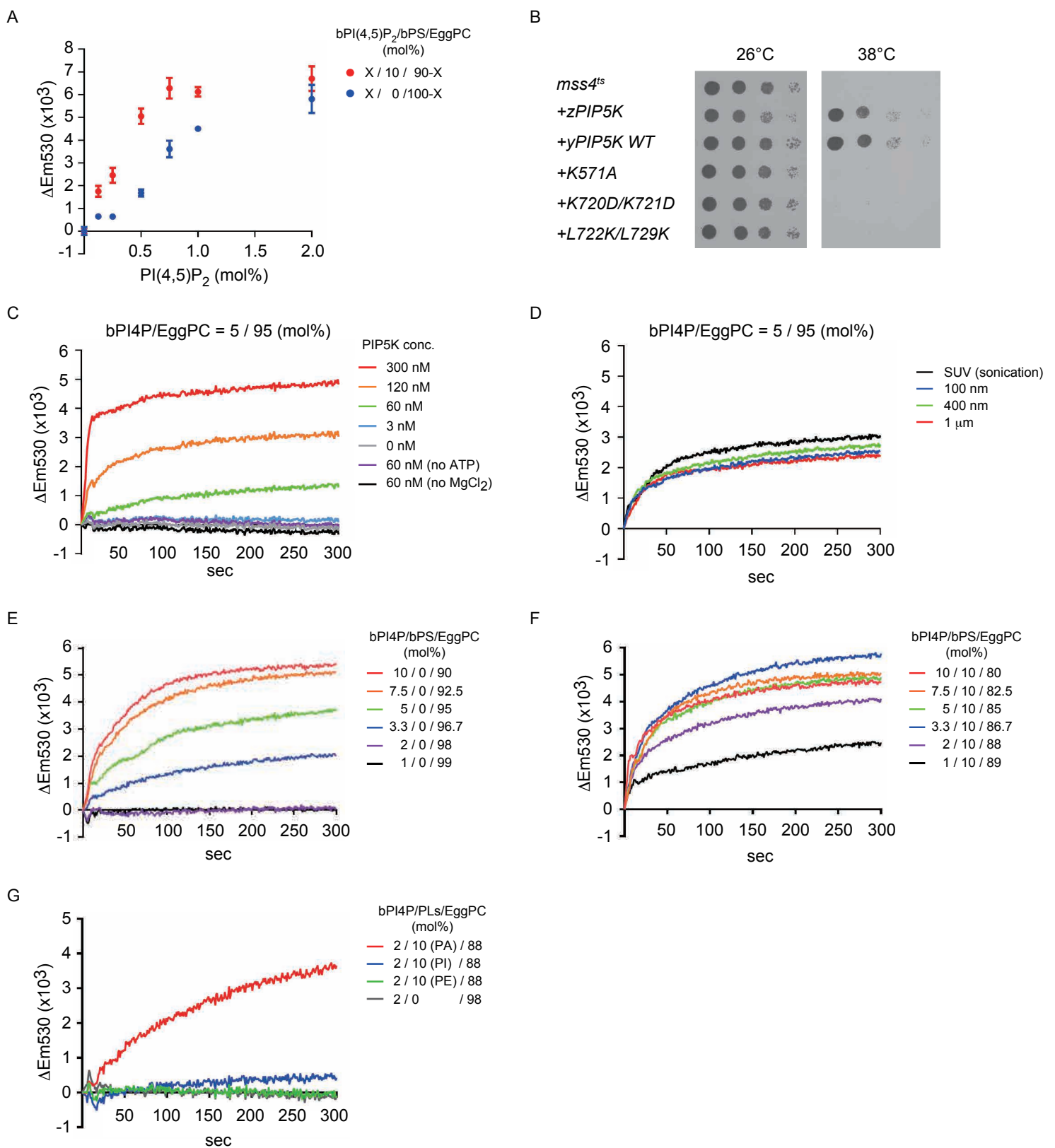


**Figure S2. PS stimulates zPIP5K activity *in vitro*, related to Figure 2**

(A) Changes in NBD-PH<sub>PLCδ</sub> fluorescence intensity in response to PI(4,5)P<sub>2</sub> levels on liposomes. Liposomes were incubated with 400 nM NBD-PH<sub>PLCδ</sub> for 5 min and NBD fluorescence was recorded by fluorescence spectroscopy. Data represent mean ± SEM (n=3). (B) Growth assay of *mss4<sup>ts</sup>* mutant cells. A zebrafish PIP5K catalytic domain (zPIP5K), a full-length yPIP5K wild-type (yPIP5K WT), a kinase dead mutant (K571A), a negatively charged mutant (K720D/K721D), an amphipathic property mutant (L722K/L729K) or empty pRS416 plasmid was expressed in *mss4<sup>ts</sup>* mutant cells as indicated. Serial dilutions of the cells were grown on -Ura plates to retain the plasmids at either 26°C or 38°C for 4 days. (C) Increase of NBD-PH<sub>PLCδ</sub> fluorescence intensity reflects PI(4,5)P<sub>2</sub> generation by the PIP 5-kinase (PIP5K) reaction. Real-time PIP5K assays were performed as described in the STAR Methods. Note that zPIP5K activity was undetectable in the absence of zPIP5K, ATP, and MgCl<sub>2</sub>. Data represent mean values (n=3; SEM<0.36x10<sup>3</sup>). (D) zPIP5K showed minimal sensitivity to differences in size of liposomes containing 5 mol% bPI4P. The indicated sizes of liposomes were obtained by extrusion. Small unilamellar vesicles (SUV) were prepared by sonication. Data represent mean values (n≥3; SEM<0.44x10<sup>3</sup>). (E, F) PIP5K activity against liposomes containing different concentrations of brain PI4P. Liposomes containing 0 mol% bPS (E) or 10 mol% bPS (F) were analyzed. (E, F) Data represent mean values (n≥3; SEM<1.07x10<sup>3</sup>). (G) The effect of phosphatidic acid (PA), phosphatidylinositol (PI) and phosphatidylethanolamine (PE) on PIP5K activity in a real-time PIP5K assay. Data represent mean values (n=3; SEM<0.64x10<sup>3</sup>).

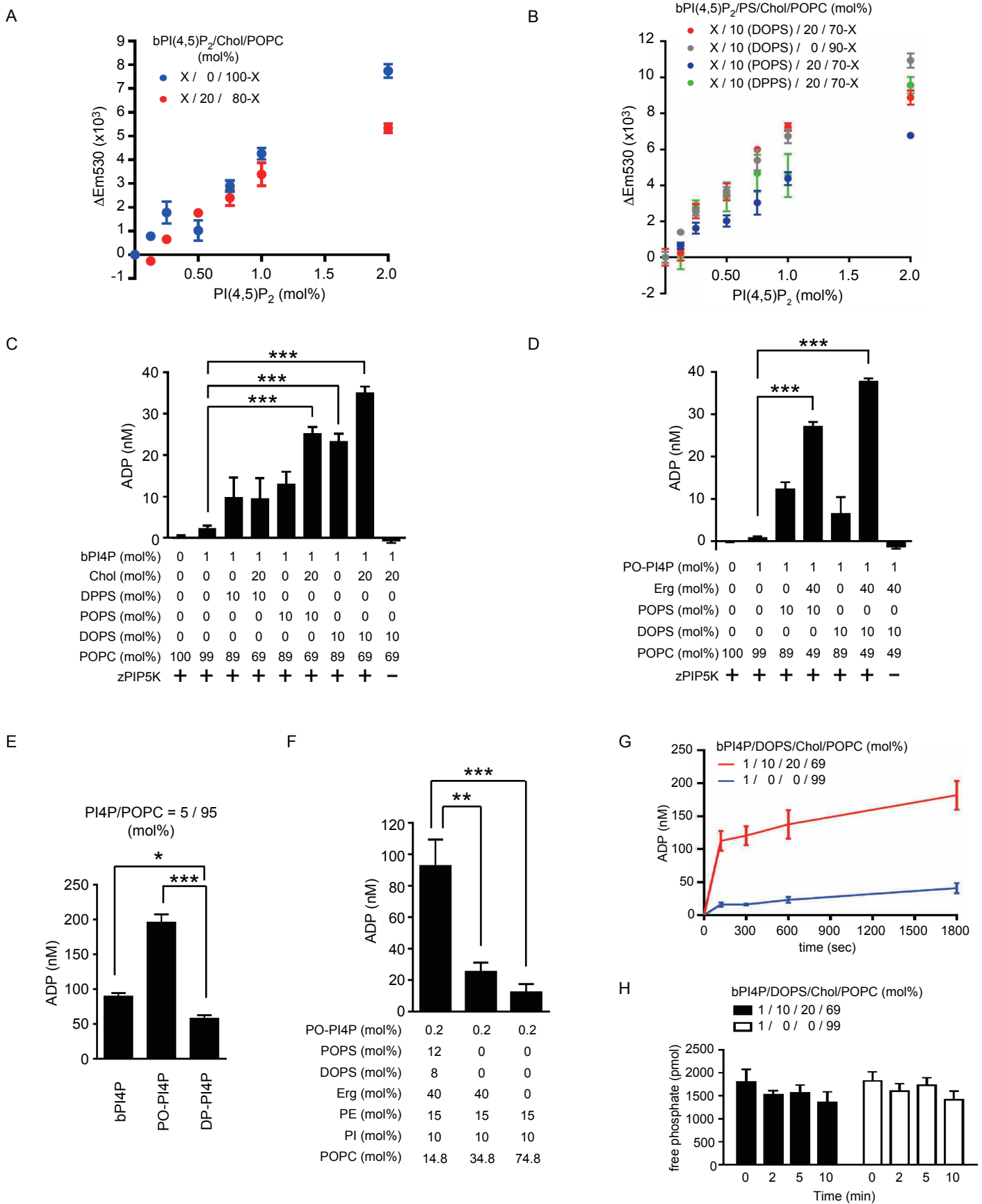


**Figure S3. Sterols stimulate zPIP5K activity *in vitro*, related to Figure 3**

(A) Effects of cholesterol on PI(4,5)P<sub>2</sub>-dose dependency of NBD-PH<sub>PLCδ</sub> fluorescence intensity. Data represent mean ± SEM (n=3).  
 (B) Calibration of effects by PS and cholesterol on NBD-PH<sub>PLCδ</sub> sensitivity to PI(4,5)P<sub>2</sub>. Data represent mean ± SEM (n=3).  
 (C) Stimulation of PIP5K activity by phosphatidylserine (PS) and cholesterol. Liposomes containing the indicated PS species and/or cholesterol were used as a substrate. After 3 min, the PIP5K reactions were stopped with ADP-Glo reagent. Data represent mean ± SEM (n = 3).  
 (D) Unsaturated PS and ergosterol (Erg) stimulate PIP5K activity. Liposomes containing various PS species and/or ergosterol as indicated were used as a substrate. After 3 min, the PIP5K reactions were stopped with ADP-Glo reagent. Data represent mean ± SEM (n = 3).  
 (E) The effect of PI4P unsaturation on zPIP5K activity. After 2 min, the PIP5K reactions were stopped with ADP-Glo reagent. Data represent mean ± SEM (n = 3). (F) ADP-Glo assay using PIP5K and liposomes resembling yeast PM lipid composition (Zinser et al., 1991) or in the absence of PS and ergosterol as indicated. After 2 min, the PIP5K reactions were stopped with ADP-Glo reagent. Data represent mean ± SEM (n = 3). (G) A time course analysis of PIP5K activity using the ADP-Glo assay. PIP5K (final conc. 130 nM) was used. Note that ADP levels rise suddenly after 120 sec in the presence of DOPS and cholesterol. Data represent mean ± SEM (n=3). (H) Free phosphate levels during the indicated PIP5K reactions were monitored over time by the Malachite Green Phosphate assay. Data represent mean ± SEM (n=3).  
 \*P < 0.05, \*\*P < 0.01, \*\*\*P < 0.001.

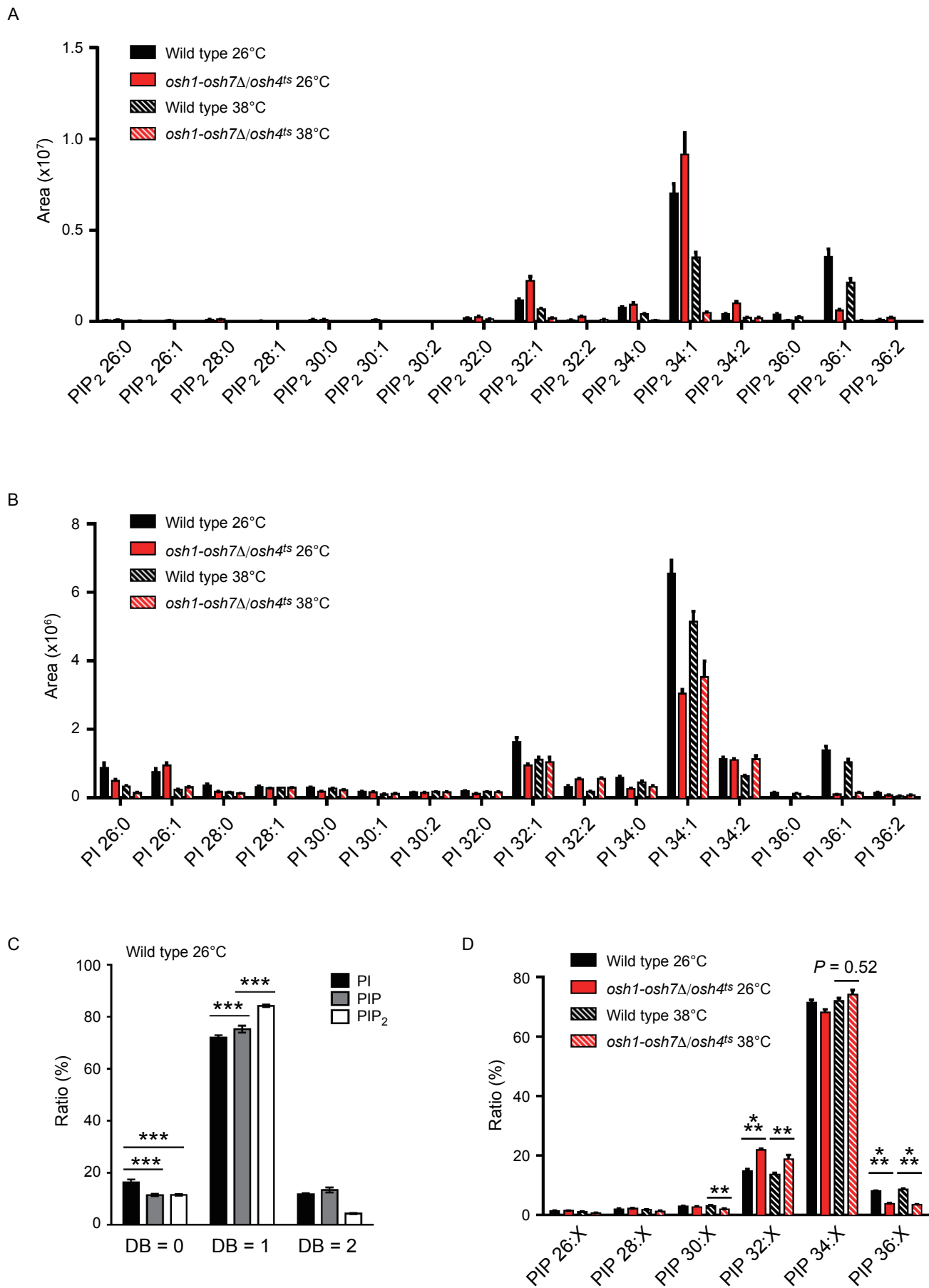


**Figure S4 The fatty acid compositions of PI, PIP and PIP<sub>2</sub> in wild type and *osh1-7Δ/osh4ts* mutant cells, related to Figure 4**  
 Analysis of PI, PIP, and PIP<sub>2</sub> levels in wild-type and *osh1-7Δ/osh4ts* cells cultured at 26°C or 38°C for 2 h by quantitative lipidomics was performed as described in the STAR Methods. (A, B) Fatty acid compositions of PIP<sub>2</sub> and PI. (C) Mono-unsaturated PIP<sub>2</sub> species are enriched in wild-type cells. (D) Fatty acid length of PIP species. (A-D) Data represent mean  $\pm$  SEM (n = 5). \*\* $P < 0.01$ , \*\*\* $P < 0.001$ .

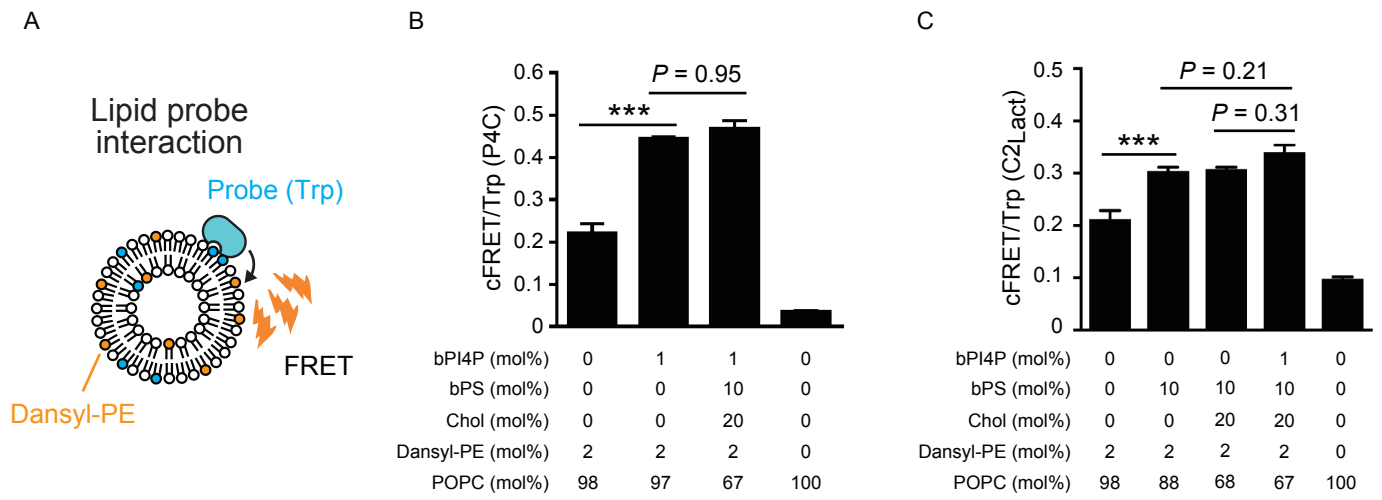


**Figure S5. Quantitative measurements of lipid probe binding in the presence of unsaturated PS, PI4P, and cholesterol, related to Figure 5**

(A) Membrane binding assay using Dansyl-PE liposomes. FRET signals increase by the proximity of dansyl-PE in the liposome to tryptophan residues in lipid probes. Corrected FRET (cFRET) was calculated as described in STAR Methods.

(B) Quantification of the PI4P probe (P4C) binding to dansyl-PE liposomes of defined compositions. (C) Quantification of PS probe (C2<sub>Lact</sub>) binding to dansyl-PE liposomes as indicated. Data represent the mean  $\pm$  SEM (n=3). \*\*\* $P < 0.001$ .

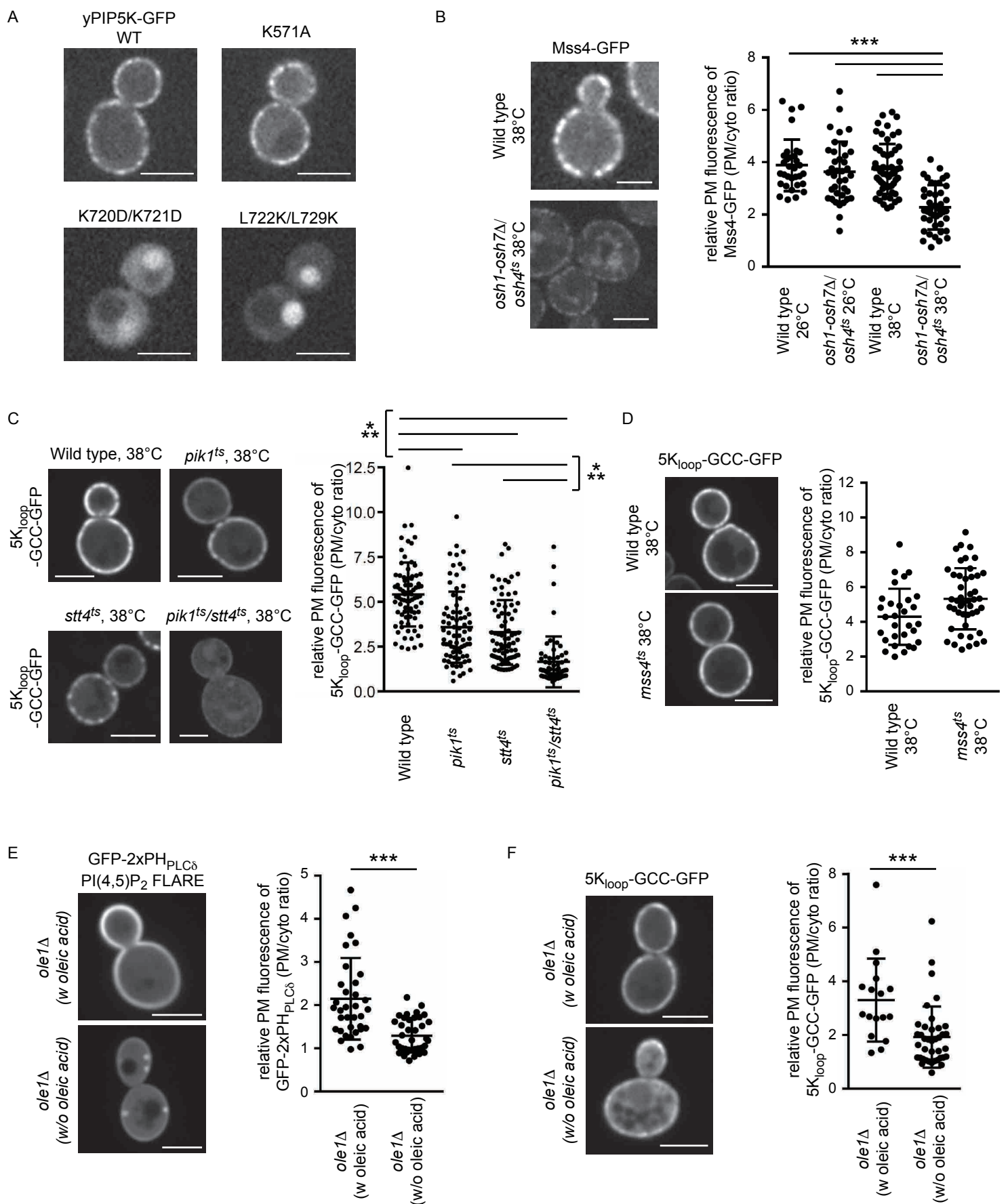


**Figure S6. Unsaturated PI4P and PS co-distribution in the PM is recognized by the specificity loop of PIP5K, related to Figure 6**

(A) Localization of GFP-tagged wild type and mutant yeast PIP5K Mss4 proteins (yPIP5K-GFP) in *mss4<sup>ts</sup>* mutant cultured at 26°C. (B) Mss4-GFP localization in wild type and *osh1-7Δ/osh4<sup>ts</sup>* cells cultured at 38°C for 2 h (left panels). Quantification of Mss4-GFP localization (PM/cyto ratio) in wild type and *osh1-7Δ/osh4<sup>ts</sup>* cells cultured at 26°C or 38°C for 2 h (right panel). Data represent mean ± SD ( $n \geq 32$  cells). (C) Localization of 5K<sub>loop</sub>-GCC-GFP in wild-type, *pik1<sup>ts</sup>*, *stt4<sup>ts</sup>* and *pik1<sup>ts</sup>/stt4<sup>ts</sup>* mutants cultured at 38°C for 1 h. (left panels). Quantification of 5K<sub>loop</sub>-GCC-GFP signals in the PM of wild-type, *pik1<sup>ts</sup>*, *stt4<sup>ts</sup>* and *pik1<sup>ts</sup>/stt4<sup>ts</sup>* mutants. Data represent mean ± SD ( $n \geq 61$  cells). (D) Quantitative analysis of 5K<sub>loop</sub>-GCC-GFP PM localization in wild type and *mss4<sup>ts</sup>* mutant cells cultured at 38°C for 1 h. Data represent mean ± SD ( $n \geq 30$  cells). (E) Quantitative localization of GFP-2xPH<sub>PLCδ</sub> in *ole1Δ* mutant cells cultured with or without 1 mM oleic acid for 20 h. Data represent mean ± SD ( $n \geq 35$  cells). (F) Quantitative localization of 5K<sub>loop</sub>-GCC-GFP in *ole1Δ* mutant cells cultured with or without 1 mM oleic acid for 20 h. Data represent mean ± SD ( $n \geq 17$  cells). Scale bars, 4 μm. \*\*\* $P < 0.001$ .

